INFECTION AND IMMUNITY, Jan. 2000, p. 247–256 Vol. 68, No. 1
0019-9567/00/$04.00+0

Delivery of CD8$^+$ T-Cell Epitopes into Major Histocompatibility Complex Class I Antigen Presentation Pathway by *Bordetella pertussis* Adenylate Cyclase: Delineation of Cell Invasive Structures and Permissive Insertion Sites

RADIM OSIČKA,[1] ADRIANA OSIČKOVÁ,[1] TÜMAY BASAR,[1] PIERRE GUERMONPREZ,[2] MARIE ROJAS,[2] CLAUDE LECLERC,[2] AND PETER ŠEBO[1]*

Cellular and Molecular Microbiology Division, Institute of Microbiology of the Academy of Sciences of the Czech Republic, CZ-142 20 Prague 4, Czech Republic,[1] and Unité de Biologie des Régulations Immunitaires, Institut Pasteur, 75724 Paris, France[2]

Received 26 July 1999/Returned for modification 2 September 1999/Accepted 19 October 1999

Bordetella pertussis **adenylate cyclase (AC) toxin-hemolysin (ACT-Hly) can penetrate a variety of eukaryotic cells. Recombinant AC toxoids have therefore been recently used for delivery of CD8$^+$ T-cell epitopes into antigen-presenting cells in vivo and for induction of protective antiviral, as well as therapeutic antitumor cytotoxic T-cell responses. We have explored the carrier potential of the ACT molecule by insertional mutagenesis scanning for new permissive sites, at which integration of two- to nine-residue-long peptides does not interfere with membrane interaction and translocation of ACT. A model CD8$^+$ T-cell epitope of ovalbumin was incorporated at 10 of these permissive sites along the toxin molecule, and the capacity of ACT constructs to penetrate into cell cytosol and deliver the epitope into the major histocompatibility complex (MHC) class I antigen processing and presentation pathway was examined. While all six constructs bearing the epitope within the Hly portion of ACT failed to deliver the epitope to the MHC class I molecules, all four toxoids with inserts within different permissive sites in the AC domain efficiently delivered the epitope into this cytosolic pathway, giving rise to stimulation of a specific CD8$^+$ T-cell hybridoma. The results suggest that, in contrast to the AC domain, the hemolysin moiety of ACT does not reach the cytosolic entry of the MHC class I pathway.**

The *Bordetella pertussis* RTX (for repeat in toxin family protein) adenylate cyclase toxin (ACT, adenylate cyclase-hemolysin [AC-Hly], or CyaA) can penetrate into a variety of immune effector cells, where upon activation by calmodulin, it catalyzes conversion of cellular ATP to cyclic AMP (cAMP) and interferes with cellular signaling and microbicidal functions (9, 26). AC toxoids with disrupted catalytic activity are, however, still cell invasive and are becoming a potent new tool for delivery of vaccinal CD8$^+$ T-cell epitopes (recognized by CD8$^+$ cytotoxic T lymphocytes) into cytosol of major histocompatibility complex (MHC) class I antigen-presenting cells. Indeed, recombinant AC toxoids have been successfully used for antigen delivery and induction of protective antiviral, as well as therapeutic antitumor CD8$^+$ cytotoxic T-cell responses in mice (11, 12, 16, 32, 33).

Translocation of the AC domain into cells is poorly understood, and whether some other portions of the ACT molecule also penetrate into cell cytosol was unknown. ACT is a large 1,706-residue-long toxin consisting of an amino-terminal AC domain of 400 residues and an RTX moiety of 1,306 residues, that can form small cation-selective membrane channels and exhibits some hemolytic activity (4, 6, 13, 28, 36). This Hly moiety itself consists of an hydrophobic channel-forming domain (residues 500 to 700) (6), of the characteristic calcium-binding RTX nonapeptide repeats, rich in glycine and aspartate residues (last 700 residues) (10, 29, 38) and of a fatty acylation domain (residues 700 to 1000), where the essential posttranslational activation by amide-linked palmitoylation of lysine 983 is taking place in the presence of the accessory acyltransferase, CyaC (1, 17). The entire and acylated AC-Hly fusion is needed for AC delivery into target cells (20, 30), while the membrane insertion and channel-forming (hemolytic) activities of the toxin do not require the AC domain and are entirely located at the Hly moiety (20, 30). ACT can penetrate directly across the cytoplasmic membrane of cells and/or erythrocytes without the need for endocytosis (5, 14). The translocation path of the AC domain across target membrane, however, does not appear to involve the hemolytic channel (6), and translocation of the AC into cells and formation of the membrane channels appear to be two independent membrane activities of ACT (7, 15, 18, 27, 29). Indirect evidence suggests that the AC domain might be delivered into cells by ACT monomers, while formation of ACT channels might require oligomerization (3, 7, 15, 18, 20, 27, 28). Structural data on ACT are, however, missing because of the size of ACT (177.6 kDa) and due to the tendency of ACT to rapidly aggregate and lose the cell-invasive activity in solutions that do not contain high concentrations of chaotropic agents.

Further progress in understanding the topology and mechanisms of membrane insertion and translocation of ACT will largely depend on the use of site-specifically-tagged toxin molecules. Identification of permissive sites for insertion into ACT of epitope tags recognized by monoclonal antibodies and insertion of unique cysteine residues along the ACT molecule, allowing its site-specific labeling with thiol-reactive probes are, therefore, of importance for generation of suitable tools for structure-function studies on ACT. In parallel, identification of such permissive sites is important for further development of the ACT as a new carrier molecule for delivery of vaccinal epitopes. In this study, we have used random linker insertion

* Corresponding author. Mailing address: Institute of Microbiology CAS, Vídeňská 1083, CZ-142 20 Prague 4, Czech Republic. Phone: (4202) 475 2762. Fax: (4202) 472 2257. E-mail: sebo@biomed.cas.cz.

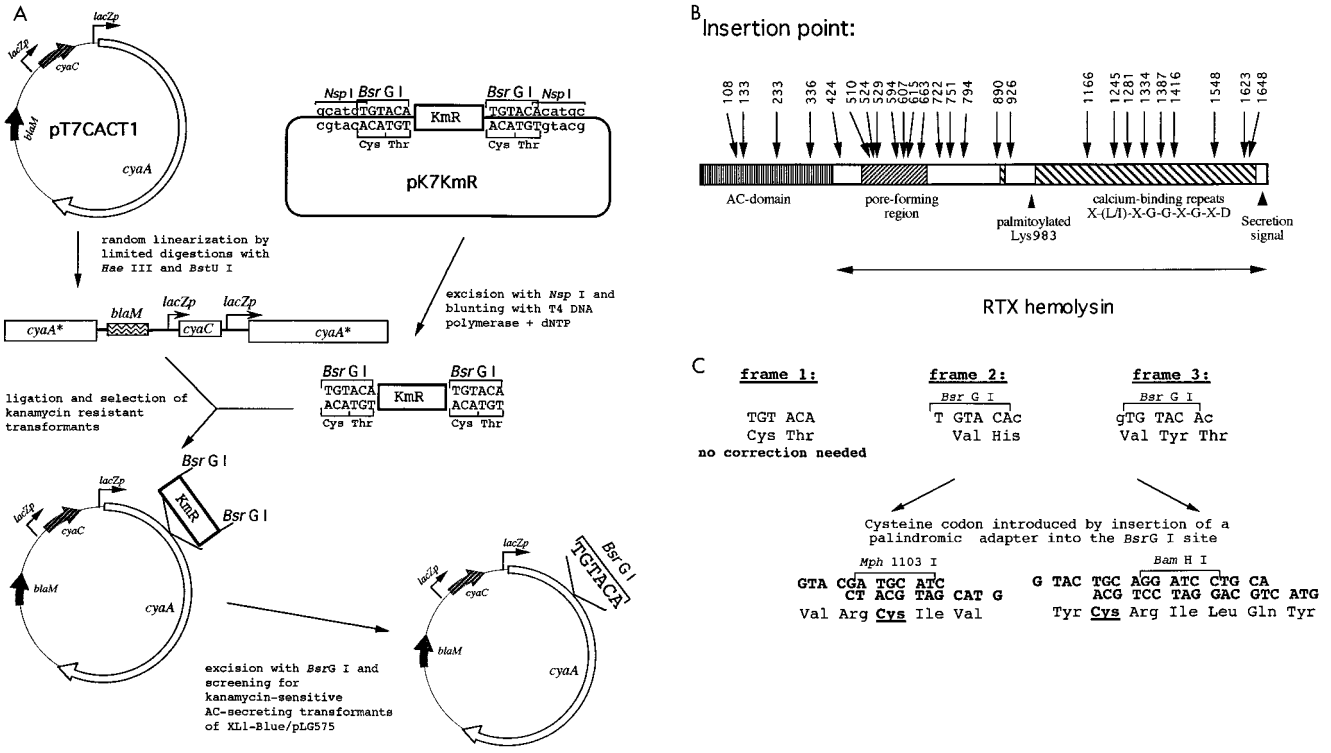

FIG. 1. Insertional mutagenesis of *cyaA*. (A) Schematic description of the employed linker insertion mutagenesis procedure. The gene denominations are as follows: *lacZp*, *lacUV5* promoter operator sequence derived from pTZ19R (Pharmacia); *blaM*, β-lactamase gene conferring ampicillin resistance; *cyaC*, gene for the accessory protein CyaC required for posttranslational activation of ACT by covalent palmitoylation at lysine 983; *cyaA*, gene for the ACT protoxin; KmR, cartridge containing the kanamycin resistance gene from pUC4K (Pharmacia). (B) Schematic depiction of the location of the characterized insertions within the ACT polypeptide, with respect to its functional domains. The numbers indicate the residues at which the various peptides described in the text were placed. (C) Representation of the outcome of insertion of the TGTACA oligonucleotide in the three possible reading frames into *cyaA*. Unique cysteine codons were introduced at the level of the unique *Bsr*GI sites with TGTACA linkers in frames 2 and 3, by insertion of a palindromic adapter encoding a hexapeptide or a nonapeptide comprising a cysteine codon.

mutagenesis to map sites along the ACT molecule, where the above-mentioned structural alterations can be performed and foreign peptides can be placed without interfering with toxin function. As a first approach to the elucidation of ACT membrane topology, the obtained mutant ACTs were used to delineate portions of ACT that are capable of delivering epitopes into the cytosolic MHC class I presentation pathway.

MATERIALS AND METHODS

Bacterial strains, growth conditions, and plasmids. The *Escherichia coli* strain XL1-Blue (Stratagene) was used throughout this work for DNA manipulation and for expression of ACT. Bacteria were grown at 37°C in Luria-Bertani medium supplemented with 150 μg of ampicillin, 30 μg of chloramphenicol, and/or 200 μg of kanamycin per ml when appropriate.

pT7CACT1 (Fig. 1A) is a construct with enhanced expression of *cyaC* and *cyaA* genes in *E. coli* under control of the isopropyl-β-D-thiogalactopyranoside (IPTG)-inducible *lacZp* promoter, which was derived from pCACT3 (7). To construct pT7CACT1, first the *cyaC* open reading frame (ORF) was amplified by PCR with purpose-designed primers 5′-GCGCGCGCCATATGCTTCCGTCC GCCCAAG and 5′-CCCGGGGGATCCTTAGGCGGTGCCCCGCGGTCG, respectively. The PCR product was fused to the translational enhancement and initiation signals of gene 10 from phage T7, by being cloned into the *Nde*I and *Bam*HI sites of pT7-7 (37). The absence of undesired mutations was verified by sequencing, and the *Xba*I fragment containing the gene together with the expression signals was inserted into a blunted *Hin*dIII site of pDLACT1 (7), to substitute for the *cyaC* allele in pCACT3, thereby placing it under *lacZp* control and yielding pT7CACT1.

pKmR-*Bsr*GI was used for preparation of the Km^r BsrG mutagenic cassette. It was constructed as follows. First, the *Bam*HI site was removed from pTZ19R (Pharmacia) by digestion with *Bam*HI and *Eco*RI, blunting of the ends with T4 DNA polymerase in presence of deoxynucleoside triphosphate (dNTP), and religation, yielding pTZΔ*Bam*HI. Second, a double-stranded adapter, obtained by self-annealing of the oligonucleotide 5′-TGTACAGGATCCTGTACACA TG, was introduced into the *Sph*I site of pTZΔ*Bam*HI, by insertion of a new *Bam*HI site flanked by two *Bsr*GI and *Nsp*I sites, respectively, yielding pTZ*Bsr*GI. Third, a *Bam*HI-excised fragment of pUC4K (Pharmacia), containing the Km^r gene for kanamycin resistance, was inserted into the *Bam*HI site of pTZ*Bsr*GI to yield pKmR-*Bsr*GI. From this plasmid, the blunt-ended Km^r-BsrG cassette, flanked by the TGTACA *Bsr*GI sites, was obtained by *Nsp*I excision and T4 DNA polymerase treatment in the presence of dNTP (Fig. 1A).

Insertional mutagenesis of pT7CACT1. The insertional mutagenesis with the Km^r-BsrG cassette is explained in detail in Fig. 1A and was done by standard procedures for DNA manipulation in vitro (31). The plasmid for expression of CyaC-activated ACT (pT7CACT1) was randomly linearized by limited digestions with the *Hae*III and *Bst*UI enzymes, cutting the G:C-rich *cyaA* DNA at 69 and 68 sites, respectively. Linearized pT7CACT1 was purified by preparative agarose gel electrophoresis, and the plasmid was recircularized with the purpose-designed mutagenic cassette Km^r-BsrG, containing a kanamycin resistance gene flanked by *Bsr*GI restriction site. About 5,000 kanamycin-resistant transformants were selected, and their plasmid DNA was pooled. The kanamycin resistance gene was then excised with *Bsr*GI, leaving in the mutagenized plasmids a randomly inserted hexanucleotide linker, TGTACA, and introducing a unique *Bsr*GI site. The insertion points were mapped by restriction analysis and determined by DNA sequencing. For this purpose, the Km^r-BsrG cassette was reintroduced into the unique *Bsr*GI sites of the plasmids from chosen mutants by using selection for gain of kanamycin resistance. Sequencing was performed with double-stranded miniprep DNA by using the Thermosequenase cycle sequencing kit (Amersham) and ^{32}P-terminally-labeled primers 5′-CAATGTAACATCAG AGATTT and 5′-ATGAGTCAGCAACACCTTCTT, respectively, which are complementary to 3′ and 5′ ends of the Km^r-BsrG cassette.

The sequencing revealed that due to a size very close to that of the singly-cut plasmid, some pT7CACT1 fragments cut at two closely adjacent sites were not separated from the linearized pT7CACT1 by agarose gel electrophoresis and also yielded several in-frame deletion constructs.

Insertion of hexa- or nonapeptides with unique cysteine residues. Unique cysteine codons were introduced at the *Bsr*GI sites of the mutant pT7CACT1 plasmids by replacing the Km^r-BsrG cassette with purpose-designed and cysteine-encoding palindromic adapters (Fig. 1C), obtained by self-annealing of synthetic oligonucleotides (5′-GTACGATGCATC and 5′-GTACTGCAGG ATCCTGCA, respectively). Plasmids with the inserted adapters were readily

identified by screening for sensitivity to kanamycin and gain of one of the new adapter-born restriction sites for *Mph*1103I and *Bam*HI, respectively. Restoration of the reading frame upon adapter insertion was verified by assay for AC secretion (see below) and verification of expression of the full-length toxin by sodium dodecyl sulfate-polyacrylamide gel electrophoresis (SDS-PAGE). The exact sequence of all inserts was verified by DNA sequencing of the respective constructs.

Insertion of OVA epitope sequences into ACT. Three double-stranded synthetic oligonucleotides encoding the ovalbumin (OVA) epitope in the required reading frames were used for insertion into the unique *Bsr*GI sites generated within the *cyaA* gene by linker mutagenesis (see above). The oligonucleotide pairs 5′-GTACTTCAATAATTAATTTCGAAAAGCTTC and 5′-GTACGAAGCTTTTCGAAATTAATTATTGAA, 5′-GTACTCAATAATTAATTTCGAAAAGCTTCA and 5′-GTACTGAAGCTTTTCGAAATTAATTATTGA, and 5′-GTACTCTCAATAATTAATTTCGAAAAGCTTCA and 5′-GTACAAGCTTTTCGAAATTAATTATTGAGA, respectively, were designed (i) to introduce a unique *Hin*dIII restriction site for rapid identification of insertion clones, (ii) to stop ACT synthesis when inserted in the inverted orientation, and (iii) to destroy the original *Bsr*GI insertion site upon ligation. The oligonucleotide sequences encoded the K^b-restricted $CD8^+$ T-cell epitope SIINFEKL corresponding to residues 257 to 264 of OVA plus flanking residues, as indicated in Table 2. The orientation and exact sequence of all inserted oligonucleotides were verified by DNA sequencing. After the cell-invasive activity of the generated ACT-OVA fusions was characterized, according to their AC activity, the constructs were detoxified by ablation of their catalytic activity. For this purpose, a synthetic *Bam*HI linker, 5′GGATCC, encoding a dipeptide, GlyPhe, was inserted into the *Eco*RV site between codons 188 and 189 of *cyaA*, and this resulted in destruction of the ATP binding site of the resulting ACT and loss of all AC activity, as described previously (12, 16).

AC secretion assay. Because the *cyaBDE* gene products which account for ACT secretion in *Bordetella* do not, for some unknown reason, constitute a functional apparatus for secretion of ACT in the heterologous *E. coli* host, the *hlyBD* genes were used for secretion of ACT. pT7CACT1 derivatives were transformed into XL1-Blue bearing the compatible plasmid pLG575 with genes encoding the HlyBD proteins of the HlyA translocator (25). Secreted AC activity was determined in cell supernatants of 2-ml overnight cultures of the individual transformants as previously described (35).

Screening for production of active ACT. We have previously shown that preparations which are suitable for reliable determination of ACT activities are obtained by 8 M urea extraction of cell debris after sonication of IPTG-induced cells (20, 34). Therefore, 5-ml cultures of the individual *E. coli* transformants were grown to mid-exponential phase and induced for ACT production by addition of 1 mM IPTG for 4 h. Accumulated ACT was extracted from cell pellets with 8 M urea–50 mM Tris-HCl (pH 8.0)–0.2 mM $CaCl_2$ upon ultrasonic disruption in an icewater bath. The crude extracts were cleared by centrifugation and used for determination of cell-invasive AC activity.

Standard techniques. SDS-PAGE analysis, determination of protein concentration, and in vitro DNA manipulations were performed according to standard protocols (31).

Characterization, production, and purification of the CyaA-derived proteins. For characterization and purification, the wild-type ACT and the different mutant derivatives were produced upon IPTG induction (1 mM) in liquid cultures in the presence of the activating protein CyaC by using *E. coli* XL1-Blue (Stratagene) and the respective constructs derived from pT7CACT1. For activity determinations, urea extracts were prepared from individual 50-ml cultures, and their ACT concentrations were equalized on the basis of the AC enzyme content, as previously described (20). For protein purification, 500-ml cultures were processed. The urea extracts of insoluble cell debris after sonication were prepared in 8 M urea–50 mM Tris-HCl (pH 8.0)–0.2 mM $CaCl_2$, as described previously (34). When appropriate, 10 mM β-mercaptoethanol was added to extraction buffer in order to prevent formation of disulfide bonds of the cysteine-containing ACT variants. Some of the proteins were further purified by ion-exchange chromatography on DEAE-Sepharose (Pharmacia) as described previously (30). For the purpose of epitope delivery tests, an additional hydrophobic chromatography purification step on phenyl-Sepharose was added (2). In the final step, the proteins were eluted with 8 M urea–50 mM Tris-HCl (pH 8.0)–10 mM β-mercaptoethanol (when appropriate) and stored at −20°C. The activities of the purified proteins were compared with toxin activities determined with the initial urea extracts. As expected, when expressed as milliunits of internalized AC enzyme per unit of AC added to cells, both types of toxin preparations exhibited very similar toxin activities, for all mutant proteins tested (Table 1). These results confirm that, as previously observed with intact ACT (20, 34), the urea extracts can be used for activity screening and characterization of the mutant ACTs without the need for purification.

Assay of AC, cell binding, and invasive and hemolytic activities. AC activities were measured as previously described in the presence of 1 μM calmodulin (22). One unit of AC activity corresponds to 1 μmol of cAMP formed per min at 30°C (pH 8.0). Because alterations outside the AC domain do not affect the specific AC activity (35), concentrations of mutant ACTs in the extracts were equalized on the basis of their AC content prior to activity testing. For constructs bearing inserts in the catalytic domain at positions 107 and 335, which had markedly reduced or nil AC-specific activity, the concentration of the ACT in extracts was adjusted by comparison of the band intensities on SDS-PAGE in the extracts. Purified proteins were tested at equal AC and/or total protein concentrations. Cell-invasive AC was determined as previously described (5), by determining the AC enzyme activity that reached the intracellular location within erythrocytes after 30 min of incubation, and was, hence, protected against externally added trypsin. To circumvent any potential differential effect on the specific AC activity of intact AC and of the AC variants altered by peptide insertion by the presence of membranes, the translocation of the AC enzyme into cells was not determined by measuring the amount of cAMP that had accumulated inside toxin-treated cells. Instead, the cell-associated (bound) AC and/or AC internalized into cells was determined upon solubilization of cell membranes in buffer containing 0.1% Triton X-100 and subsequent dilution of the extracted enzyme in a reaction mixture containing 0.1% Triton X-100 and saturating concentrations of ATP and the activator calmodulin under first-order kinetics conditions in the absence of membranes (5). The hemolytic activity was determined as hemoglobin release upon incubation of the toxins for 270 min with washed sheep erythrocytes at 5×10^8 cells per ml (5). Erythrocyte binding of the toxins was determined as described in detail previously (20).

In vitro assay for MHC class I presentation of the ACT-OVA constructs. The stimulation of B3Z cells, a $CD8^+$ T-cell hybridoma specific for the SIINFEKL–H-$2K^b$ complex, was monitored by interleukin 2 (IL-2) release in the supernatants of cultures in the presence of antigen-presenting cells (APCs) (21). B3Z cells (10^5 cells/well) were cocultured in flat-bottom 96-well culture plates for 18 h in the presence of various ACT concentrations and splenocytes (which originated from C57BL/6 mice, 6 to 8 weeks old; Janvier, France) as APCs (10^5/well) in a 200-μl final volume of complete medium (RPMI 1640 supplemented with 10% fetal calf serum, 2 mM L-glutamine, 10^{-5} M 2-mercaptoethanol, 100 U of penicillin per ml, and 100 μg of streptomycin per ml). After 18 h, the supernatants were harvested and frozen for at least 2 h at −70°C. Then, 10^4 cells of the cytotoxic T-lymphocyte CTLL cell line per well, a line which proliferates specifically in response to IL-2, were cultured with 100 μl of supernatant in a 0.2-ml final volume (8). Two days later, [^{3}H]thymidine (NEN Life Science, Boston, Mass.) was added, and the cells were harvested 18 h later with an automated cell harvester (Skatron, Lier, Norway). Incorporated thymidine was detected by scintillation counting. In all experiments, each point was done at least in duplicate and more often in triplicate. Results are expressed in Δcpm (cpm in the presence of ACT − cpm in the absence of ACT). It has been verified that treatment of splenocytes with detoxified ACT alone did not induce any production of IL-2 (data not shown).

RESULTS AND DISCUSSION

Insertional mutagenesis of ACT. The ACT molecule was scanned for permissive peptide insertion sites by linker insertion mutagenesis of its structural gene, *cyaA* (Fig. 1), and functional characterization of the obtained mutant ACT. In order to allow straightforward mutagenesis of the large, 5.1-kb-long *cyaA* gene, a purpose-designed and excisable mutagenic cassette carrying the gene for resistance to kanamycin (Km^r) was employed (23). The cassette was modified so that, upon excision, it left at the insertion site a hexanucleotide, TGTACA (Fig. 1A), corresponding to a unique *Bsr*GI restriction site and encoding a di- or tripeptide insert, depending on the respective reading frame at the insertion point. This procedure enabled antibiotic resistance selection of insertion mutants, rapid sequencing of all insertion points with a single pair of primers matching the ends of the mutagenic cassette, and a high-throughput antibiotic sensitivity screening for replacement of the mutagenic cassette with an oligonucleotide of choice.

The expression and restoration of a full-length *cyaA* reading frame upon excision of the mutagenic cassette were verified for 400 kanamycin-sensitive clones, by screening them for HlyBD-TolC-dependent secretion of ACT into culture supernatants (35). This allowed elimination of clones with mutations abolishing expression of ACT, as well as clones with frameshift mutations in *cyaA*, which yielded truncated toxins lacking the carboxy-terminal secretion signal. The selection of mutants was further narrowed by screening 150 clones for cell-invasive AC toxin activity in extracts of IPTG-induced cells. A subset of 55 active and 2 inactive mutant ACTs was chosen for determination of the linker insertion points by DNA sequencing, and 27 sequence-characterized mutant proteins (Fig. 1B) were subjected to further characterization (Table 1). In this set, two

TABLE 1. Characteristics of the mutant ACTs with di- or tripeptide and cysteine peptide inserts

Protein[a]	Insert[b]	% Activity vs wild type	
		Invasive[c,d]	Hemolytic[c]
Di- or tripeptide inserts			
ACT wild type	None	100 ± 11	100 ± 15
ACT108/VH	Gly^{107}**VH** His^{108}	98 ± 12	101 ± 14
ACT133/VYT	Met^{132}**VYT** Asp^{134}	96 ± 10	97 ± 15
ACT233/VH	Gly^{232}**VH** Leu^{233}	101 ± 13	102 ± 13
ACT336/VH	Gly^{335}**VH** Gln^{336}	97 ± 11	98 ± 9
ACT424/VYT	Met^{423}**VYT** Ala^{425}	99 ± 12	97 ± 12
ACTΔ510–515/VYT	Glu^{509}**VYT** Glu^{516}	75 ± 9	230 ± 45
ACT524/VH	Arg^{523}**VH** Gly^{524}	60 ± 8	60 ± 9
ACT529/VYT	Trp^{528}**VYT** Gly^{530}	65 ± 8	75 ± 9
ACT594/CT*	Ala^{593}***CT*** Arg^{594}	98 ± 13	96 ± 14
ACT607/VYT	Ser^{606}**VYT** Gly^{608}	96 ± 11	99 ± 12
ACTΔ615–655/VYT	Leu^{614}**VYT** Gln^{656}	<1	<2
ACTΔ663–688/VYT	Thr^{662}**VYT** Ser^{689}	0	0
ACT722/VYT	Leu^{721}**VYT** Asn^{723}	29 ± 4	23 ± 4
ACT751/VYT	Leu^{750}**VYT** Asn^{752}	101 ± 13	97 ± 14
ACT794/VYT	Asn^{793}**VYT** Asp^{795}	37 ± 6	38 ± 6
ACT890/VYT	Leu^{889}**VYT** Lys^{891}	96 ± 12	99 ± 14
ACT926/CT*	Ser^{925}***CT*** Arg^{926}	102 ± 14	95 ± 13
ACT1166/VH	Gly^{1165}**VH** Arg^{1166}	69 ± 7	52 ± 7
ACTΔ1245–1273/VYT	Ser^{1244}**VYT** Gln^{1274}	27 ± 4	22 ± 3
ACT1281/VH	Gly^{1280}**VH** Gln^{1281}	42 ± 6	37 ± 5
ACT1334/VH	Gly^{1333}**VH** Gln^{1334}	100 ± 12	96 ± 14
ACTΔ1387–1407/VYT	Glu^{1386}**VYT** Asp^{1408}	93 ± 13	98 ± 13
ACT1387/VYT	Glu^{1386}**VYT** Gly^{1388}	100 ± 14	97 ± 11
ACT1416/VYT	Gln^{1415}**VYT** Asn^{1417}	79 ± 9	78 ± 10
ACT1548/VH	Gly^{1547}**VH** Leu^{1548}	71 ± 9	65 ± 8
ACT1623/VYT	Phe^{1622}**VYT** Arg^{1624}	88 ± 7	91 ± 7
ACT1648/VH	Arg^{1647}**VH** Asp^{1648}	99 ± 14	92 ± 9
Cysteine peptide inserts			
ACT108/E2-Cys*	**VR*C*IVH**	100 ± 12	100 ± 15
ACT133/E3-Cys*	**VY*C*RILQYT**	96 ± 13	101 ± 13
ACT233/E2-Cys	**VR*C*IVH**	98 ± 12	104 ± 15
ACT336/E2-Cys	**VR*C*IVH**	ND[e]	99 ± 14
ACT424/E3-Cys*	**VY*C*RILQYT**	101 ± 14	96 ± 12
ACTΔ510–515/E3-Cys*	**VY*C*RILQYT**	<2	280 ± 53
ACT524/E2-Cys	**VR*C*IVH**	0	0
ACT529/E3-Cys*	**VY*C*RILQYT**	20 ± 3	25 ± 4
ACT607/E3-Cys*	**VY*C*RILQYT**	88 ± 9	93 ± 10
ACTΔ615–655/E3-Cys	**VY*C*RILQYT**	<1	<2
ACTΔ663–688/E3-Cys	**VY*C*RILQYT**	0	0
ACT722/E3-Cys*	**VY*C*RILQYT**	32 ± 6	27 ± 4
ACT751/E3-Cys	**VY*C*RILQYT**	101 ± 13	98 ± 14
ACT794/E3-Cys*	**VY*C*RILQYT**	27 ± 4.3	30 ± 4.8
ACT890/E3-Cys	**VY*C*RILQYT**	0	0
ACT1166/E2-Cys	**VR*C*IVH**	61 ± 7	50 ± 8
ACTΔ1245–1273/E3-Cys*	**VY*C*RILQYT**	26 ± 4	24 ± 5
ACT1281/E2-Cys	**VR*C*IVH**	28 ± 5	26 ± 4
ACT1334/E2-Cys*	**VR*C*IVH**	88 ± 10	94 ± 14
ACTΔ1387–1407/E3-Cys*	**VY*C*RILQYT**	88 ± 7	95 ± 13
ACT1387/E3-Cys*	**VY*C*RILQYT**	97 ± 12	96 ± 15
ACT1416/E3-Cys*	**VY*C*RILQYT**	81 ± 10	75 ± 9
ACT1548/E2-Cys	**VR*C*IVH**	57 ± 6	60 ± 7
ACT1623/E3-Cys	**VY*C*RILQYT**	0	0
ACT1648/E2-Cys*	**VR*C*IVH**	98 ± 13	96 ± 14

[a] The mutant ACT variants for which the toxin activities were determined with both the urea extracts and purified protein preparations are indicated by an asterisk. Δ indicates a deletion encompassing the indicated residues.

[b] Boldface characters indicate inserted amino acid residues at given positions in ACT. The inserted unique cysteine residues are indicated in italics.

[c] The activities are expressed as percentages of wild-type ACT activity and represent average values ± standard deviations from at least three independent determinations performed in duplicate with three different toxin preparations ($n = 6$).

[d] Invasive activity was determined as the AC activity translocated into sheep erythrocytes and protected against digestion by extracellularly added trypsin (5).

[e] ND, not determined.

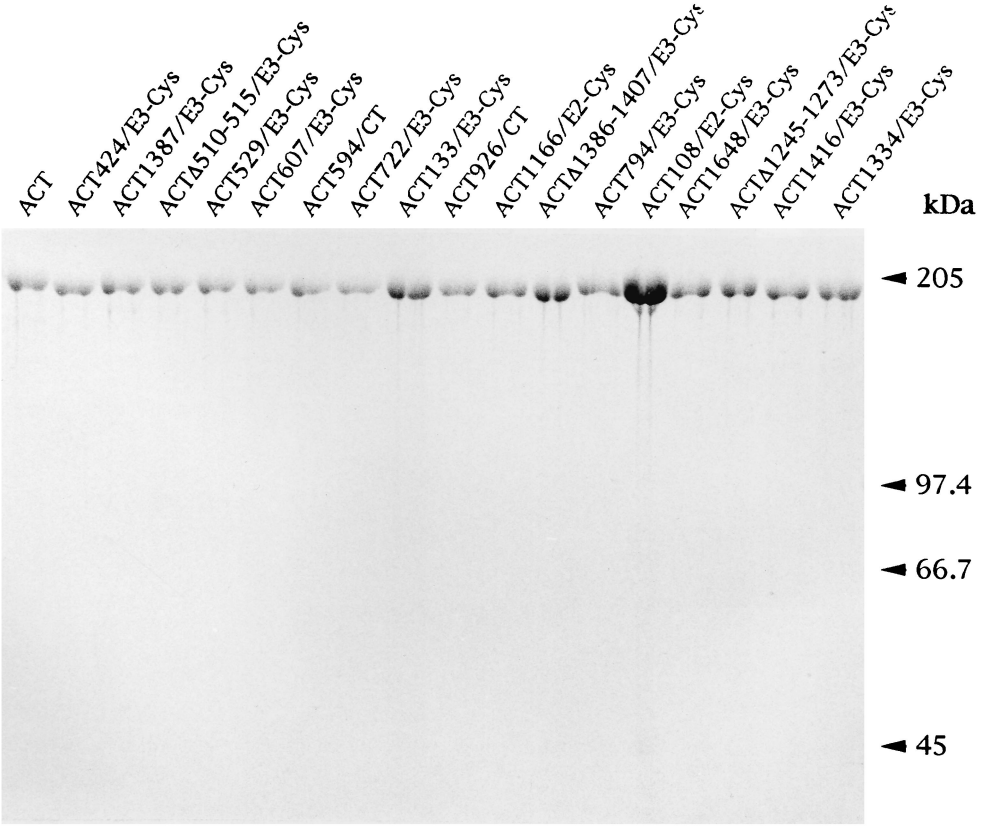

FIG. 2. SDS-PAGE analysis of the purified ACT preparations. Seventeen of 25 cysteine-containing ACT proteins were purified from urea extracts by DEAE-Sepharose chromatography as previously described (30), and 2 to 4 U of each enzyme was analyzed together with the wild-type ACT on a 7.5% acrylamide gel. It can be seen that due to reduced specific AC activity of the ACT108/E2-Cys protein, a several-fold-larger amount of this protein was loaded, compared to the amounts of the other constructs.

constructs contained a CysThr dipeptide insert, while the rest of the mutant ACTs harbored either a dipeptide insert, ValHis (VH), or a substitution of an Ala residue by the tripeptide ValTyrThr (VYT), respectively (Fig. 1C). Out of these 25 active mutant ACTs, 14 were fully active (>90% of wild-type ACT activity), 8 exhibited cell-invasive activities between 60 and 90% of wild-type ACT, and 4 mutant ACTs had activities reduced into the range of 20 to 60% of wild-type ACT (Table 1). Interestingly, one of the mutant ACTs with an insert at position 510 exhibited significantly enhanced hemolytic activity (see below).

Permissive peptide insertion sites and mutations highlighting important functional structures of ACT. It was important to test how insertion of longer peptides at defined positions will affect biological activities of ACT. Moreover, active ACT constructs with unique cysteine residue inserts would be amenable to site-specific labeling with thiol-reactive probes and subsequently serve in ACT-membrane interaction studies. Therefore, palindromic oligonucleotide adapters, encoding either a hexapeptide, VRCIVH (E2-Cys), or a nonapeptide, VYCRILQYT (E3-Cys), were inserted into the *Bsr*GI sites (Fig. 1C). Each of these longer inserts also introduced a unique cysteine residue and allowed generation of a second set of mutant toxins with cysteine residues placed at 25 different positions along the toxin (Table 1).

From the total of 27 mutant proteins with inserted unique cysteine residues, 17 mutant ACTs were purified from urea extracts by ion-exchange chromatography (Fig. 2) for further characterization. These toxins were selected either because they exhibited significant toxin activity, or because the constructs exhibited particular properties, such as the deletion construct ACTΔ510–515/E3, which exhibited enhanced hemolytic activity, or because the toxins contained the cysteine residue in a particular position interesting from the point of view of being used upon thiol-selective labeling in membrane interaction and topology studies of ACT (not described in this report). The cell-invasive and hemolytic activities of the purified proteins, per unit of AC activity added to target cells, were found to match very well the activities determined with urea extracts containing the same proteins (Table 1) and confirmed our previous observations (20, 34) that urea extracts can be used for reliable characterization of the mutant ACTs, without the need for purification.

Some of the characterized peptide insertion mutations highlighted new structures important for ACT function. At four positions where di- or tripeptide inserts were tolerated without any major effect on toxin activities, insertion of a hexa- or nonapeptide caused a complete loss of cell-invasive activity (Table 1). These sites at residues 510 and 524 of the hydrophobic domain, at residue 891 of the acylation domain, and at residue 1623 of the repeat domain, respectively, are hence nonpermissive to larger peptides and highlight new structurally sensitive and functionally important regions of ACT. The insertion points at residues 524, 891, and 1623 appear to be located within structures important for membrane interaction of the toxin, since insertion of the hexa- or nonapeptide at

these positions abolished target cell binding of the mutant toxins (data not shown).

Particularly informative, however, is the case of the ACTΔ510–515/E3-Cys construct, in which replacement of the deleted hexapeptide ASSAVA by the nonapeptide VYCRILQYT caused complete loss of invasive AC activity, while similarly to the ACTΔ510–515/VYT construct with the shorter insert, it simultaneously enhanced the specific hemolytic activity more than two times (Table 1). This result is consistent with the effects of point substitutions of the adjacent residue, Glu509, in which a proline substitution selectively ablates AC domain translocation across the cell membrane without affecting the membrane channel-forming capacity of the E509P mutant ACT. Moreover, a charge reversion at residue 509 by a lysine substitution enhances the hemolytic activity of ACT about two times (26a). Collectively these results strongly suggest that the insertion point at residue 510 is located within a structure involved in AC translocation across membrane and modulating as well the hemolytic activity of ACT.

Further information relevant for understanding the structure-function relationships within the ACT molecule can be derived from the 10 permissive insertion mutations mapping into the calcium-binding repeat domain of ACT (last 700 residues). This was found to bind up to 45 calcium ions and consists of five distinct repeat blocks, comprising a total of 17 consensus repeats of the sequence X-(L/I)-X-G-G-X-G-X-D and up to 33 additional degenerate repeats (Fig. 3) (29). The data presented in Table 1 show that some of the degenerate repeats are dispensable for ACT function. Deletions of two approximate repeats at the beginning of the repeat blocks III (residues 1245 to 1273) and IV (residues 1387 to 1407) still allowed 25% and full ACT activities, respectively. Furthermore, insertions of hexa- or nonapeptides at four positions within the repeats yielded ACTs exhibiting from 25 to 75% of toxin activities, and insertions at four other positions resulted in toxins exhibiting over 80% activity. These data demonstrate a structural flexibility of the ACT repeat domain. However, in agreement with the presumed role of consensus repeats in binding the calcium ions required for toxin activity (29), none of the permissive insertion sites was located in any of the consensus repeats of ACT.

Of interest as well are the newly identified permissive peptide insertion sites within the AC domain. Two of them were at positions 133 and 233, which are close to sites identified previously (23). A third new permissive site was identified at residue 108, where already the hexapeptide insert had caused about a fourfold reduction in specific AC activity (data not shown). The cell-invasive activity of the respective constructs, when expressed as the yield of the internalized versus input AC activity was, however, not affected by the mutations (Table 1). The fourth new site in the AC domain was at residue 336. The cell-invasive activity of the protein ACT336/E2-Cys could not, however, be determined, because its specific AC activity was below 2% of the activity of intact ACT (data not shown). Nevertheless, as described below, a construct with the OVA epitope inserted at this site efficiently delivered the OVA epitope into the MHC class I pathway, and it can therefore be assumed that insertion of peptides at position 336 does not significantly affect the cell invasiveness of the AC domain.

Delineation of cell-invasive portions of ACT suitable for delivery of foreign CD8$^+$ T-cell epitopes. Recently, the cell-invasive ACT with various peptides inserted at residue 224 of the AC domain has been successfully used for CD8$^+$ T-cell epitope delivery into the MHC class I presentation pathway and the activation of specific CD8$^+$ cytotoxic T-cell responses against tumors and viruses (11, 12, 32). The insertional mutagenesis and screening procedure described here allowed definition of a set of an additional 10 permissive sites along the entire ACT molecule, at which insertion of up to nine-residue-long peptides does not substantially alter the capacity of the toxin to penetrate into cells. It was, therefore, important to test which of the newly identified permissive sites allow CD8$^+$ T-cell epitope delivery to the MHC class I molecules. For this purpose, a model K^b-restricted CD8$^+$ T-cell epitope, SIINFEKL, corresponding to residues 257 to 264 of OVA, was inserted at 12 positions along the toxin molecule. As summarized in Table 2, eight of the constructs retained a cell-invasive capacity identical or close to that of the intact ACT, and for one construct, ACT336/OVA, the invasive activity could not be assessed because of the loss of AC activity (see below). This confirms that at least eight and potentially nine of the new sites were permissive as well to insertion of other peptides than those used for initial screening. Two additional constructs, ACT594/OVA and ACT926/OVA, respectively, exhibited a reduced or nil capacity to associate with target cells and were therefore used as convenient negative controls in the epitope delivery experiments.

Prior to their use for in vitro presentation assays, where higher ACT concentrations are used, the toxicity consisting of enzymatic AC activity of the ACT-OVA constructs (conversion of intracellular ATP to cAMP) had to be ablated in order to eliminate its potential interference with the physiology of the cells present in the assay. This was achieved by disruption of the ATP binding site in the AC domain by placing an additional dipeptide insert between residues 188 and 189 of ACT (23). The resulting toxoids, devoid of any detectable AC activity (data not shown), were purified close to homogeneity, as documented in Fig. 4. The capacity of the toxoids to deliver the inserted OVA epitope into the MHC class I antigen processing and presentation pathway was determined by measuring the capacity of APCs, which were incubated with the toxoids, to stimulate IL-2 release from the CD8$^+$ T-cell hybridoma B3Z, which selectively recognizes the complexes of the K^b MHC class I molecules with the SIINFEKL peptide at the surface of APCs (23). As shown in Fig. 5, APCs incubated with up to a 10-μg/ml concentration of all eight toxoids carrying the OVA epitope in the Hly portion failed to stimulate the B3Z cells. In contrast, the B3Z hybridoma cells were stimulated upon exposure to APCs that were treated with less than a 1-μg/ml concentration of any of the four AC toxoids carrying the OVA epitope within the AC domain. It is worth mentioning that due to the size of the toxoids carrying the integrated OVA epitope (178 kDa), the effective concentration of the epitope peptide applied to APCs was less than 6 nM. It can therefore be concluded that the constructs with the OVA epitope inserted in the AC domain delivered the epitope for antigenic presentation quite efficiently.

We have previously demonstrated that ACT-mediated delivery of CD8$^+$ T-cell epitopes for MHC class I presentation does not require endocytosis and the epitope has to follow the classical presentation pathway involving cytosolic proteasome cleavage followed by transporter of antigenic peptides (TAP)-mediated transport into endoplasmic reticulum, where the K^b-OVA complexes form and enter the vesicular transport leading to cell-surface exposition of the epitope on MHC class I molecules (16). Entry into this pathway implies, hence, that the antigen is accessible to processing within the cytosol. The results reported here show that out of 10 ACT-OVA toxoids that have retained their cell-binding capacity, only the 4 having the epitope inserted within the AC domain (residues 1 to 400) were able to deliver the epitope into the MHC class I pathway,

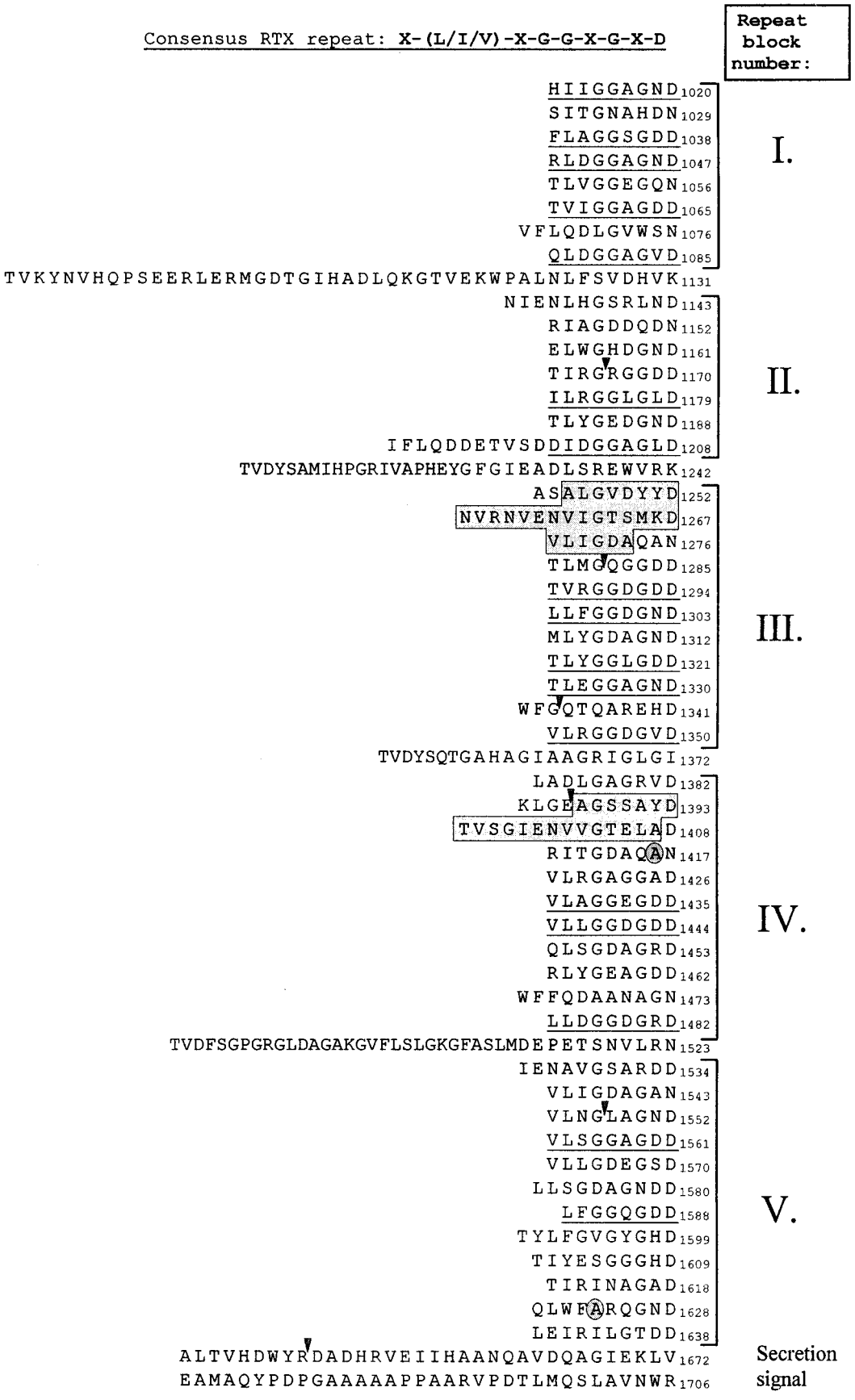

FIG. 3. Sequence of the repeat region of ACT organized in repeat blocks. The sequence representing the repeats of ACT was aligned according to the consensus repeat nonapeptide motif. The points of linker insertions within the repeat blocks are indicated by arrowheads or by an encircled residue which was substituted for by the insert. The dispensable repeat sequences, which were deleted, are boxed.

TABLE 2. Characteristics of the ACT constructs with the OVA epitope

Protein	Insertion point and flanking sequences[a]	% Activity vs wild type		
		Binding[b]	Invasive AC[b,c]	Hemolytic[b]
ACT wild type	None	100 ± 11	100 ± 12	100 ± 15
ACT108/OVA	SSLAHG^{107}**VL**SIINFEKL**VH**^{108}HTAVDL	97 ± 12	101 ± 11	95 ± 10
ACT133/OVA	GLVTGM^{132}**VY**SIINFEKL**GYT**^{134}DGVVAS	101 ± 14	98 ± 9	97 ± 12
ACT233/OVA	SEATGG^{232}**VL**SIINFEKL**VH**^{233}LDRERI	100 ± 9	96 ± 9	99 ± 14
ACT336/OVA	LKEYIG^{335}**VL**SIINFEKL**VH**^{336}QQRGEG	ND[d]	ND	96 ± 9
ACT424/OVA	GEVSDM^{423}**VY**SIINFEKL**GYT**^{425}AAVEAA	96 ± 10	97 ± 10	102 ± 11
ACT594/OVA	GDALLA^{593}**CT**SIINFEKL**RT**^{594}RGVTSG	57 ± 6	<2	14 ± 3
ACT607/OVA	QVAGAS^{606}**VY**SIINFEKL**GYT**^{608}GAAAGA	64 ± 7	66 ± 5	30 ± 4
ACT751/OVA	ARHEQL^{750}**VY**SIINFEKL**GYT**^{752}NSDGL	103 ± 11	93 ± 10	40 ± 5
ACT926/OVA	VLANAS^{925}**CT**SIINFEKL**RT**^{926}RIHYDG	0	0	0
ACT1334/OVA	GNDWFG^{1333}**VL**SIINFEKL**VH**^{1334}NTQARE	98 ± 13	102 ± 14	97 ± 14
ACT1387/OVA	VDKLGE^{1386}**VY**SIINFEKL**GYT**^{1388}GSSAYD	85 ± 9	82 ± 9	75 ± 8
ACT1648/OVA	VHDWYR^{1647}**VL**SIINFEKL-**VH**^{1648}DADHRV	97 ± 11	99 ± 12	95 ± 12

[a] The OVA epitope sequence is underlined, and the flanking residues are indicated in boldface.
[b] Expressed as a percentage of wild-type ACT activity. The activities of the proteins were determined prior to ablation of the AC activity (insertion of a dipeptide insert between residues 188 and 189) as described in Materials and Methods. The activities represent average values ± standard deviations from at least three independent determinations performed in duplicate with three different toxin preparations ($n = 6$).
[c] Invasive activity was determined as the AC activity translocated into sheep erythrocytes and protected against digestion by extracellularly added trypsin (5).
[d] ND, not determined (no measurable AC activity).

while the epitopes inserted along the Hly portion were not presented to $CD8^+$ T cells. It is important to note that the epitopes were inserted within the Hly in the same flanking residue context as within the AC domain. It can therefore be expected that, if exposed to the proteasome, they would be processed with comparable efficiency. It is also unlikely that, if internalized, the Hly moiety would be more resistant to intracytosolic proteolysis than the AC domain. The cell cytosol contains typically less than 1 μM concentrations of free Ca^{2+} ions, and under such conditions, the hemolysin part of ACT was shown to be exquisitely sensitive to proteolytic degradation in vitro (19). Moreover, the AC domain forms high-affinity

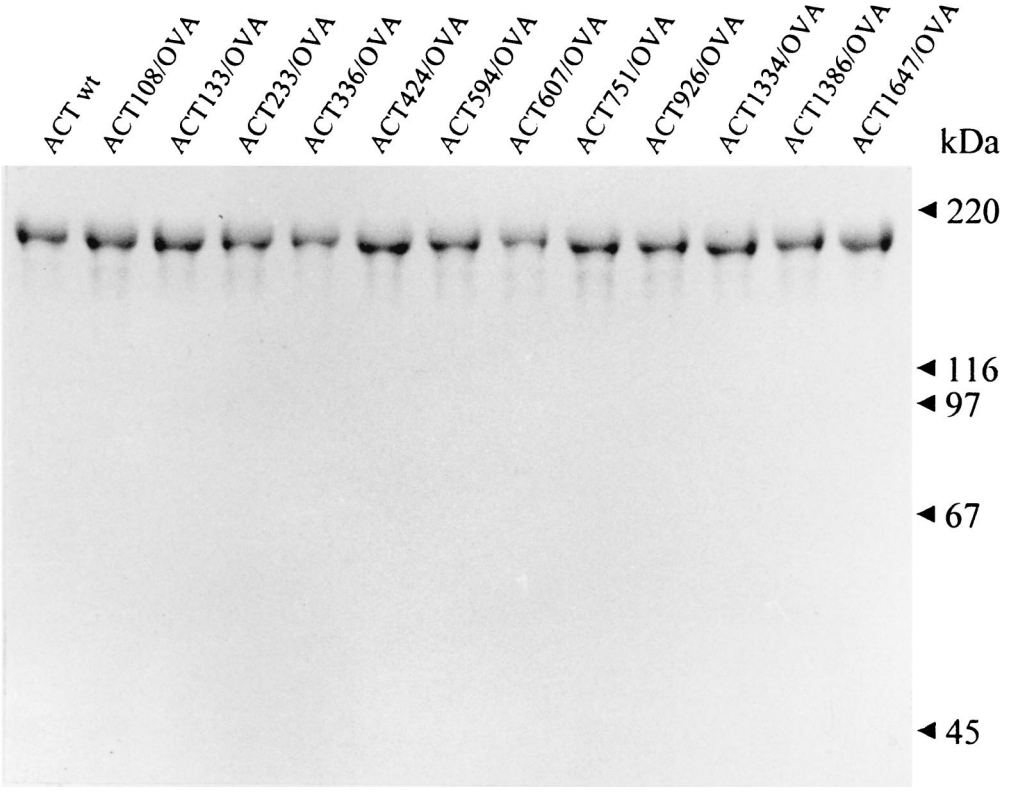

FIG. 4. SDS-PAGE analysis of the detoxified ACT-OVA preparations. The detoxified OVA-containing ACT constructs were purified from urea extracts by a combination of DEAE-Sepharose and phenyl-Sepharose chromatographies as previously described (2). One to 3 μg of each protein was analyzed on a 7.5% acrylamide gel and stained with Coomassie blue. wt, wild type.

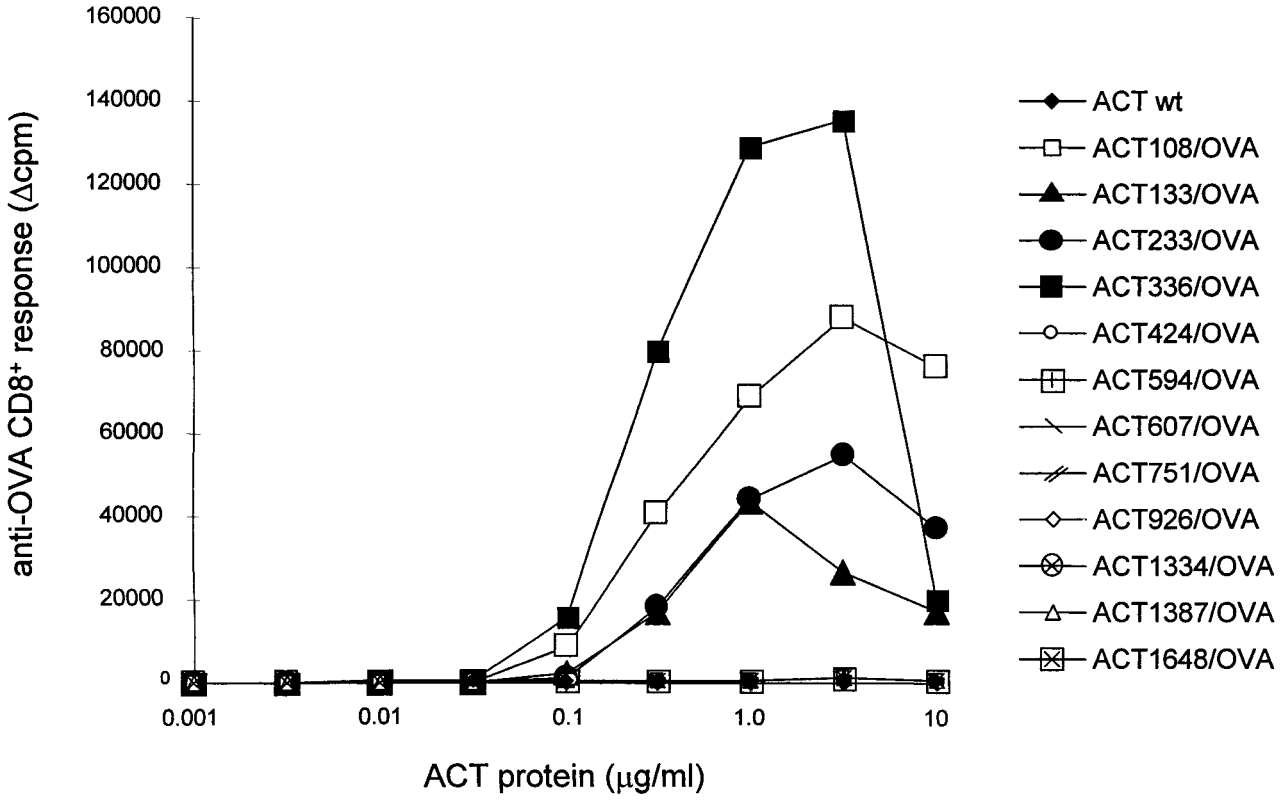

FIG. 5. Location of the $CD8^+$ T-cell epitope within ACT determines its presentation to $CD8^+$ T cells. Splenocytes used as APCs were incubated in the presence of various concentrations of the ACT proteins harboring the OVA epitope at different sites and cocultured with B3Z, an anti-OVA $CD8^+$ T-hybridoma selectively recognizing cell-surface-presented complexes of the $H\text{-}2K^b$ MHC class I molecules with bound OVA epitope (SIINFEKL). IL-2 secretion by the stimulated B3Z $CD8^+$ T cells was determined by the CTLL proliferation method. Results are expressed in Δcpm of incorporated [^{3}H]thymidine (cpm in the presence of ACT − cpm in the absence of ACT). wt, wild type.

complexes with intracellular calmodulin, which, at least in vitro, significantly increases the resistance of the AC enzyme to proteolysis (24). The AC domain would therefore be expected to be more resistant to processing than the Hly domain. Therefore, it is likely that if the Hly portion of ACT containing the OVA epitope would reach cell cytosol, it would be processed and the resulting OVA peptide would be presented and detected on cell surface, as were the epitopes inserted in the AC domain. Collectively, the results presented here indicate that only the AC domain of ACT reaches the site of proteasome processing in the cytosol, while the Hly portion remains membrane associated and/or extracytosolic, thereby rendering the epitopes inserted within the Hly moiety inaccessible to processing for MHC class I presentation.

Concluding remarks. We report here the identification and use of a set of new permissive peptide insertion sites along the ACT molecule. This enabled insertion of peptides containing unique cysteine residues at 20 different positions of ACT, where these peptides mostly had a minor or undetectable effect on ACT activities and are amenable to site-specific tagging at the cysteine residues with thiol-reactive probes for toxin-membrane interaction studies. Furthermore, the identified permissive sites within all functional domains have now allowed construction of ACT molecules tagged with epitopes recognized by commercially available monoclonal antibodies and their use for analysis of ACT topology within target membranes (J. Loucká et al., unpublished data).

As a first approach to analyzing ACT membrane topology, the ACT portions that can enter cell cytosol and deliver a model $CD8^+$ T-cell epitope into the MHC class I antigen processing and presentation pathway were mapped here. The results suggest that, in contrast to the AC domain, the hemolysin moiety does not reach the cytosolic entry of this pathway. The new sites permissive for insertion of heterologous peptides into the Hly moiety, however, open the way toward construction of toxins with epitopes inserted in extracytosolic and membrane-associated domains of ACT, which as a result of natural membrane recycling, might potentially direct $CD4^+$ T-cell epitopes for processing into endosomes and for subsequent presentation on MHC class II molecules.

It should be mentioned that we have recently obtained a strong antibody response against B-cell epitopes inserted within ACT at some of the permissive sites identified here (T. Basar et al., unpublished data). Hence, hybrid toxins carrying multiple epitopes at different sites along the ACT molecule can now be easily constructed and tested as a polyvalent antigen carrier, capable of simultaneous stimulation of both cellular immunity (cytotoxic T lymphocyte) and humoral immune responses.

ACKNOWLEDGMENTS

The help of Jiří Mašín, Jiřina Loucká, and Valeria Sheshko with protein purification and toxin assays; stimulating discussions with Daniel Ladant and Agnes Ullmann; and the gift of pTZΔBamHI from Josette Pidoux are gratefully acknowledged.

This work was supported by grants 310/98/0432 from the Grant Agency of the Czech Republic, A5020907 from the Grant Agency of the Academy of Sciences, and VS96149 and ME167 from the Ministry

of Education Youth and Sports of the Czech Republic to P.S. and by grants from Agence Nationale de la Recherche sur le SIDA (ANRS) and Association pour la Recherche sur le Cancer (ARC) to C.L.

REFERENCES

1. **Barry, E. M., A. A. Weiss, I. E. Ehrmann, M. C. Gray, E. L. Hewlett, and M. St. Mary Goodwin.** 1991. *Bordetella pertussis* adenylate cyclase toxin and hemolytic activities require a second gene, *cyaC*, for activation. J. Bacteriol. **173:**720–726.
2. **Basar, T., V. Havlíček, S. Bezoušková, P. Halada, M. Hackett, and P. Šebo.** 1999. The conserved lysine 860 in the additional fatty-acylation site of *Bordetella pertussis* adenylate cyclase toxin is crucial for toxin function independently of its acylation status. J. Biol. Chem. **274:**10777–10783.
3. **Bejerano, M., M. Nisan, A. Ludwig, W. Goebel, and E. Hanski.** 1999. Characterization of the C-terminal domain essential for toxic activity of adenylate cyclase toxin. Mol. Microbiol. **31:**381–392.
4. **Bellalou, J., D. Ladant, and H. Sakamoto.** 1990. Synthesis and secretion of *Bordetella pertussis* adenylate cyclase as a 200-kilodalton protein. Infect. Immun. **58:**1195–2000.
5. **Bellalou, J., H. Sakamoto, D. Ladant, C. Geoffroy, and A. Ullmann.** 1990. Deletions affecting hemolytic and toxin activities of *Bordetella pertussis* adenylate cyclase. Infect. Immun. **58:**3242–3247.
6. **Benz, R., E. Maier, D. Ladant, A. Ullmann, and P. Šebo.** 1994. Adenylate cyclase toxin (CyaA) of *Bordetella pertussis*: evidence for the formation of small ion-permeable channels and comparison with HlyA of *Escherichia coli*. J. Biol. Chem. **269:**27231–27239.
7. **Betsou, F., P. Šebo, and N. Guiso.** 1993. CyaC-mediated activation is important not only for toxic but also for protective activities of *Bordetella pertussis* adenylate cyclase-hemolysin. Infect. Immun. **61:**3583–3589.
8. **Bottomly, K., L. Davis, and P. Lipsky.** 1991. Measurement of human and murine interleukin 2 and interleukin 4, p. 6.3.1. *In* A. M. Kruisbeck, J. E. Coligan, D. H. Margulis, E. M. Shevach, and W. Strober (ed.), Current protocols in immunology. Wiley, New York, N.Y.
9. **Confer, D. L., and J. W. Eaton.** 1982. Phagocyte impotence caused by an invasive bacterial adenylate cyclase. Science **217:**948–950.
10. **Coote, J. G.** 1992. Structural and functional relationships among the RTX toxin determinants of Gram-negative bacteria. FEMS Microbiol. Rev. **88:** 137–162.
11. **Fayolle, C., D. Ladant, G. Karimova, A. Ullmann, and C. Leclerc.** 1999. Therapy of murine tumors with recombinant *Bordetella pertussis* adenylate cyclase toxins carrying a cytotoxic T cell epitope. J. Immunol. **162:**4157–4162.
12. **Fayolle, C., P. Šebo, D. Ladant, A. Ullmann, and C. Leclerc.** 1996. In vivo induction of CTL responses by recombinant adenylate cyclase of *Bordetella pertussis* carrying viral $CD8^+$ T cell epitopes. J. Immunol. **156:**4697–4706.
13. **Glaser, P., D. Ladant, O. Sezer, F. Pichot, A. Ullmann, and A. Danchin.** 1988. The calmodulin-sensitive adenylate cyclase of *Bordetella pertussis*: cloning and expression in *Escherichia coli*. Mol. Microbiol. **2:**19–30.
14. **Gordon, V. M., W. W. Young, Jr., S. M. Lechler, M. C. Gray, S. H. Leppla, and E. L. Hewlett.** 1989. Adenylate cyclase toxins from *Bacillus anthracis* and *Bordetella pertussis*. Different processes for interaction with and entry into target cells. J. Biol. Chem. **264:**14792–14796.
15. **Gray, M., G. Szabo, A. Otero, L. Gray, and E. Hewlett.** 1998. Distinct mechanisms for K^+ efflux, intoxication, and hemolysis by *Bordetella pertussis* AC toxin. J. Biol. Chem. **273:**18260–18267.
16. **Guermonprez, P., D. Ladant, G. Karimova, A. Ullmann, and C. Leclerc.** 1999. Direct delivery of the *Bordetella pertussis* adenylate cyclase toxin to the MHC class I antigen presentation pathway. J. Immunol. **162:**1910–1916.
17. **Hackett, M., L. Guo, J. Shabanowitz, D. F. Hunt, and E. L. Hewlett.** 1994. Internal lysine palmitoylation in adenylate cyclase toxin from *Bordetella pertussis*. Science **266:**433–435.
18. **Hackett, M., C. B. Walker, L. Guo, M. C. Gray, C. S. Van, A. Ullmann, J. Shabanowitz, D. F. Hunt, E. L. Hewlett, and P. Šebo.** 1995. Hemolytic, but not cell-invasive activity, of adenylate cyclase toxin is selectively affected by differential fatty-acylation in *Escherichia coli*. J. Biol. Chem. **270:**20250–20253.
19. **Hewlett, E. L., L. Gray, M. Allietta, I. E. Ehrmann, V. M. Gordon, and M. C. Gray.** 1991. Adenylate cyclase toxin from *Bordetella pertussis*. Conformational change associated with toxin activity. J. Biol. Chem. **266:**17503–17508.
20. **Iwaki, M., A. Ullmann, and P. Šebo.** 1995. Identification by in vitro complementation of regions required for cell-invasive activity of *Bordetella pertussis* adenylate cyclase toxin. Mol. Microbiol. **17:**1015–1024.
21. **Karttunen, J., S. Sanderson, and N. Shastri.** 1992. Detection of rare antigen-presenting cells by the lacZ T cell activation assay suggests an expression cloning strategy for T cell antigens. Proc. Natl. Acad. Sci. USA **89:**6020–6024.
22. **Ladant, D.** 1988. Interaction of *Bordetella pertussis* adenylate cyclase with calmodulin: identification of two separated calmodulin-binding domains. J. Biol. Chem. **263:**2612–2618.
23. **Ladant, D., P. Glaser, and A. Ullmann.** 1992. Insertional mutagenesis of *Bordetella pertussis* adenylate cyclase. J. Biol. Chem. **267:**2244–2250.
24. **Ladant, D., S. Michelson, R. S. Sarfati, A.-M. Gilles, R. Predeleanu, and O. Bârzu.** 1989. Characterization of the calmodulin-binding and of the catalytic domains of *Bordetella pertussis* adenylate cyclase. J. Biol. Chem. **264:**4015–4020.
25. **Mackman, N., J.-M. Nicaud, L. Gray, and I. B. Holland.** 1985. Genetical and functional organisation of the *Escherichia coli* haemolysin determinant 2001. Mol. Gen. Genet. **201:**282–288.
26. **Mock, M., and A. Ullmann.** 1993. Calmodulin-activated bacterial adenylate cyclases as virulence factors. Trends Microbiol. **1:**187–192.

26a. **Osičková, A., et al.** J. Biol. Chem., in press.

27. **Rogel, A., and E. Hanski.** 1992. Distinct steps in the penetration of adenylate cyclase toxin of *Bordetella pertussis* into sheep erythrocytes. Translocation of the toxin across the membrane. J. Biol. Chem. **267:**22599–22605.
28. **Rogel, A., R. Meller, and E. Hanski.** 1991. Adenylate cyclase toxin from *Bordetella pertussis*. The relationship between induction of cAMP and hemolysis. J. Biol. Chem. **266:**3154–3161.
29. **Rose, T., P. Šebo, J. Bellalou, and D. Ladant.** 1995. Interaction of calcium with *Bordetella pertussis* adenylate cyclase toxin. Characterization of multiple calcium-binding sites and calcium-induced conformational changes. J. Biol. Chem. **270:**26370–26376.
30. **Sakamoto, H., J. Bellalou, P. Šebo, and D. Ladant.** 1992. *Bordetella pertussis* adenylate cyclase toxin. Structural and functional independence of the catalytic and hemolytic activities. J. Biol. Chem. **267:**13598–13602.
31. **Sambrook, J., E. F. Fritsch, and T. Maniatis.** 1989. Molecular cloning: a laboratory manual, 2nd ed. Cold Spring Harbor Laboratory Press, Cold Spring Harbor, N.Y.
32. **Saron, M. F., C. Fayolle, P. Šebo, D. Ladant, A. Ullmann, and C. Leclerc.** 1997. Anti-viral protection conferred by recombinant adenylate cyclase toxins from *Bordetella pertussis* carrying a CD8+ T cell epitope from lymphocytic choriomeningitis virus. Proc. Natl. Acad. Sci. USA **94:**3314–3319.
33. **Šebo, P., C. Fayolle, O. d'Andria, D. Ladant, C. Leclerc, and A. Ullmann.** 1995. Cell-invasive activity of epitope-tagged adenylate cyclase of *Bordetella pertussis* allows in vitro presentation of a foreign epitope to $CD8^+$ cytotoxic T cells. Infect. Immun. **63:**3851–3857.
34. **Šebo, P., P. Glaser, H. Sakamoto, and A. Ullmann.** 1991. High-level synthesis of active adenylate cyclase toxin of *Bordetella pertussis* in a reconstructed *Escherichia coli* system. Gene **104:**19–24.
35. **Šebo, P., and D. Ladant.** 1993. Repeat sequences in the *Bordetella pertussis* adenylate cyclase toxin can be recognized as alternative carboxy-proximal secretion signals by the *Escherichia coli* alpha-haemolysin translocator. Mol. Microbiol. **9:**999–1009.
36. **Szabo, G., M. C. Gray, and E. L. Hewlett.** 1994. Adenylate cyclase toxin from *Bordetella pertussis* produces ion conductance across artificial lipid bilayers in a calcium and polarity-dependent manner. J. Biol. Chem. **269:**22496–22499.
37. **Tabor, S., and C. Richardson.** 1985. A bacteriophage T7 RNA polymerase/promoter system for controlled exclusive expression of genes. Proc. Natl. Acad. Sci. USA **82:**1074–1078.
38. **Welch, R. A.** 1991. Pore-forming cytolysins of gram-negative bacteria. Mol. Microbiol. **5:**521–528.

Editor: J. T. Barbieri